

AnalogCoder-Pro: Unifying Analog Circuit Generation and Optimization via Multi-modal LLMs

Yao Lai¹, Souradip Poddar², Sungyoung Lee², Guojin Chen³, Mengkang Hu¹,
Bei Yu³, Ping Luo¹, and David Z. Pan²

¹Department of Computer Science, The University of Hong Kong

²Department of Electrical and Computer Engineering, The University of Texas at Austin

³Department of Computer Science and Engineering, The Chinese University of Hong Kong

pluo@cs.hku.hk, dpan@ece.utexas.edu

Abstract—Despite advances in analog design automation, analog front-end design still heavily depends on expert intuition and iterative simulations, underscoring critical gaps in fully automated optimization for performance-critical applications. Recently, the rapid development of Large Language Models (LLMs) has brought new promise to analog design automation. However, existing work remains in its early stages, and holistic joint optimization for practical end-to-end solutions remains largely unexplored. We propose AnalogCoder-Pro, a unified multimodal LLM-based framework that integrates generative capabilities and optimization techniques to jointly explore circuit topologies and optimize device sizing, automatically generating performance-specific, fully sized schematic netlists. AnalogCoder-Pro employs rejection sampling for fine-tuning LLMs on high-quality synthesized circuit data and introduces a multimodal diagnosis and repair workflow based on functional specifications and waveform images. By leveraging LLMs to interpret generated circuit netlists, AnalogCoder-Pro automates the extraction of critical design parameters and the formulation of parameter spaces, establishing an end-to-end workflow for simultaneous topology generation and device sizing optimization. Extensive experiments demonstrate that these orthogonal approaches significantly improve the success rate of analog circuit design and enhance circuit performance. The codes and dataset are released at github.com/laiyao1/AnalogCoderPro.

I. INTRODUCTION

Automating analog front-end design has long faced significant challenges. This is largely due to the intricate interplay of underlying circuit physics in deep submicron technologies and the complex, multidimensional performance trade-offs [1]–[3]. As a result, design flows remain heavily reliant on expert heuristics and extensive simulation cycles, limiting both efficiency and scalability. Modern device sizing algorithms [4]–[11] aim to improve sample efficiency, but are largely restricted to predefined architectures. Meanwhile, topology exploration faces several critical barriers, including time-consuming simulation-in-the-loop [12], [13], reliance on expert-driven equation formulation [14]–[16], limited topological diversity [17], class-specific algorithm design [18], and risks to structural validity [19]. Moreover, existing workflows often decouple topology exploration and circuit sizing into separate sequential stages, leading to suboptimal results and costly redesign cycles when post-hoc parameter tuning cannot compensate for inherent topological limitations. Re-

Table I: Comparison of Works

Work	Multiple Types ¹	Verified FT Data ²	MLM Debug ³	Circuit Gen.	Circuit Opt.	Open-Source
CktGNN [22]		•		•	•	•
LADAC [23]	•				•	
ADO-LLM [24]	•				•	
LaMAGIC [25], [26]				•	•	
AnalogCoder [27]	•		○	•		
SPICEPilot [28]	•		○	•		
LEDRO [29]				•		
Aritsan [30]				•	•	
AmpAgent [31]				•	•	
Atelier [32]				•	•	
AnalogXpert [33]				•		
Malasa-Chai [34]	•	○		•		
AnalogGenie [21], [35]	•	○		•	•	
AnalogFed [36]	•			•	•	
AnalogCoder-Pro	•	•	•	•	•	•

¹ Whether the work supports multiple circuit type designs.

² • - Functionality verified fine-tuning circuit data; ○ - Not explicitly verified.

³ • - Full multi-modal debugging capability by signal images (e.g., waveform, frequency response), ○ - Text-only debugging.

alizing that practical applications require performance-driven co-optimization of topology and design parameters, recent approaches have emerged [20], [21]. However, while the method in [20] enables automated circuit synthesis, it requires substantial upfront effort in repository setup and simulation infrastructure, limiting its applicability to topology selection from a predefined library. AnalogGenie [21] enables end-to-end topology generation by pre-training on various circuit types and fine-tuning on specific categories. However, it still requires manual data collection and separate fine-tuning for each class, which limits its scalability. These limitations underscore the need for a holistic co-design framework that can generalize across circuit types and seamlessly integrate performance-driven topology generation and circuit sizing with minimal human intervention, ultimately enabling more practical and scalable automated analog design.

The advent of Large Language Models (LLMs) has ushered in powerful generative capabilities in circuit design, demonstrating immense potential in RTL-based digital design [37]–[45] and TCL-based EDA flow script generation [46]. However, given the complex circuit-specific physics combined with the lack of standardized domain-specific training corpora, analog design automation applications remain in their early stages,

as shown in Table I. Current efforts can be categorized into two primary directions: topology generation via code or netlist synthesis [27], [28], [33], [34], and LLM-accelerated circuit sizing [23], [24], [30]–[32]. While these approaches show promise, critical limitations persist. First, **the importance of verified, high-quality fine-tuning data is often underappreciated**. For example, AnalogGenie [21] and Masala-Chai [34] provide netlist data but do not fully incorporate practical functional verification. Without ensuring the correctness of netlists, the reliability of downstream tasks, such as fine-tuning LLMs, can be significantly compromised. Second, **current approaches have yet to adequately leverage the potential of multimodal large language models (MLLMs)**. While debugging circuits through waveform analysis is often more intuitive and insightful than relying solely on textual or numerical data, waveform understanding is rarely integrated into the design process. This omission limits the ability of MLLMs to address tasks requiring a deeper understanding of circuit behavior. Consequently, the untapped potential for a unified, end-to-end framework enabling performance-driven co-optimization of analog front-end design remains an open challenge.

To address these challenges, we propose AnalogCoder-Pro, a unified MLLM-based framework that integrates circuit generation and optimization. The framework features: (1) functional verification of synthesized circuit data using rejection sampling, which ensures high-quality data for effective fine-tuning; (2) MLLM-guided circuit debugging based on waveform image analysis; and (3) LLM-assisted parameter and search space extraction, enabling a fully automated design flow from high-level requirements to functionally verified and optimized circuit netlists, as shown in Fig. 2.

The main contributions of this work include:

- To address data scarcity, we leverage MLLMs to generate circuit netlists from schematic diagrams and automatically verify their functionality via simulation, enabling effective rejection sampling fine-tuning with a small amount of verified data.
- We utilize MLLMs to analyze malfunctioning circuit waveforms, as waveform images provide more intuitive and informative features than numerical data or text, enabling the model to identify and fix circuit design errors more effectively.
- We integrate LLM-based parameter extraction with automatic sizing based on the optimizer, and combine them with LLM-generated circuit netlists to establish a fully automated, end-to-end analog circuit design flow. Users only need to input high-level design requirements.
- Extensive experiments on multiple analog circuit types show that our approach consistently outperforms existing baselines in both success rate and performance.

II. PRELIMINARIES

A. Analog Circuit Design

Analog circuit design is one of the most intricate stages in the integrated circuit (IC) flow, involving both front-end and

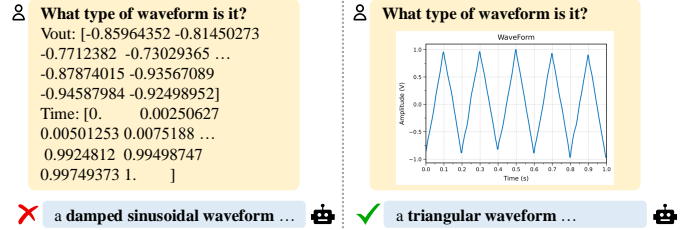


Fig. 1: **LLMs vs. MLLMs in Waveform Identification.** LLMs using textual data (left) misidentify a noisy triangular waveform, whereas MLLMs, given the waveform image (right), correctly recognize its type.

back-end tasks. In the front-end, designers must synthesize suitable topologies and optimize device parameters to meet stringent, often conflicting performance criteria such as gain, bandwidth, and power consumption. Achieving a high figure-of-merit (FoM) requires navigating large, high-dimensional design spaces and managing complex trade-offs, further complicated by the strong coupling between topology and sizing decisions, where an optimal choice in one aspect may be suboptimal in another. The back-end translates these logical designs into manufacturable layouts [47]–[50], ensuring process compliance.

Recent advances in artificial intelligence have brought new tools to analog design, including reinforcement learning [4], [6], [51], graph-based generative models [22], [52], and language model-based approaches [11], [23], [24], [27]–[29], [31], [33], [34]. Nevertheless, many of these techniques tackle topology generation and parameter optimization in isolation, which can result in incompatibilities that hinder overall performance and necessitate iterative redesigns.

To mitigate these issues, recent research has explored unified frameworks that jointly consider topology and sizing. AnalogGenie [21], [35] first pre-trains on a manually collected set of circuit topologies, then fine-tunes the model specifically on high-performance topologies. The method in [20] automatically ranks candidate topologies according to user requirements, then performs sizing and verification on each, but remains limited to a predefined set of topologies. Artisan [30] focuses on behavioral-level synthesis for op-amps design, omitting device-level refinement. Thus, despite these advances, a truly scalable, general-purpose methodology for end-to-end, performance-driven analog design automation remains elusive.

B. Rejection Sampling Fine-tuning

Rejection Sampling (RS) is a straightforward and effective technique for improving the quality of generation tasks. The core idea is to have the model produce multiple candidate solutions for a given problem, and then apply a scoring mechanism, such as simulation results, unit tests, or expert evaluation, to filter these candidates, retaining only the best-performing ones for subsequent model fine-tuning. By learning primarily from high-quality solutions, the model incrementally improves its ability to generate desirable results in future tasks.

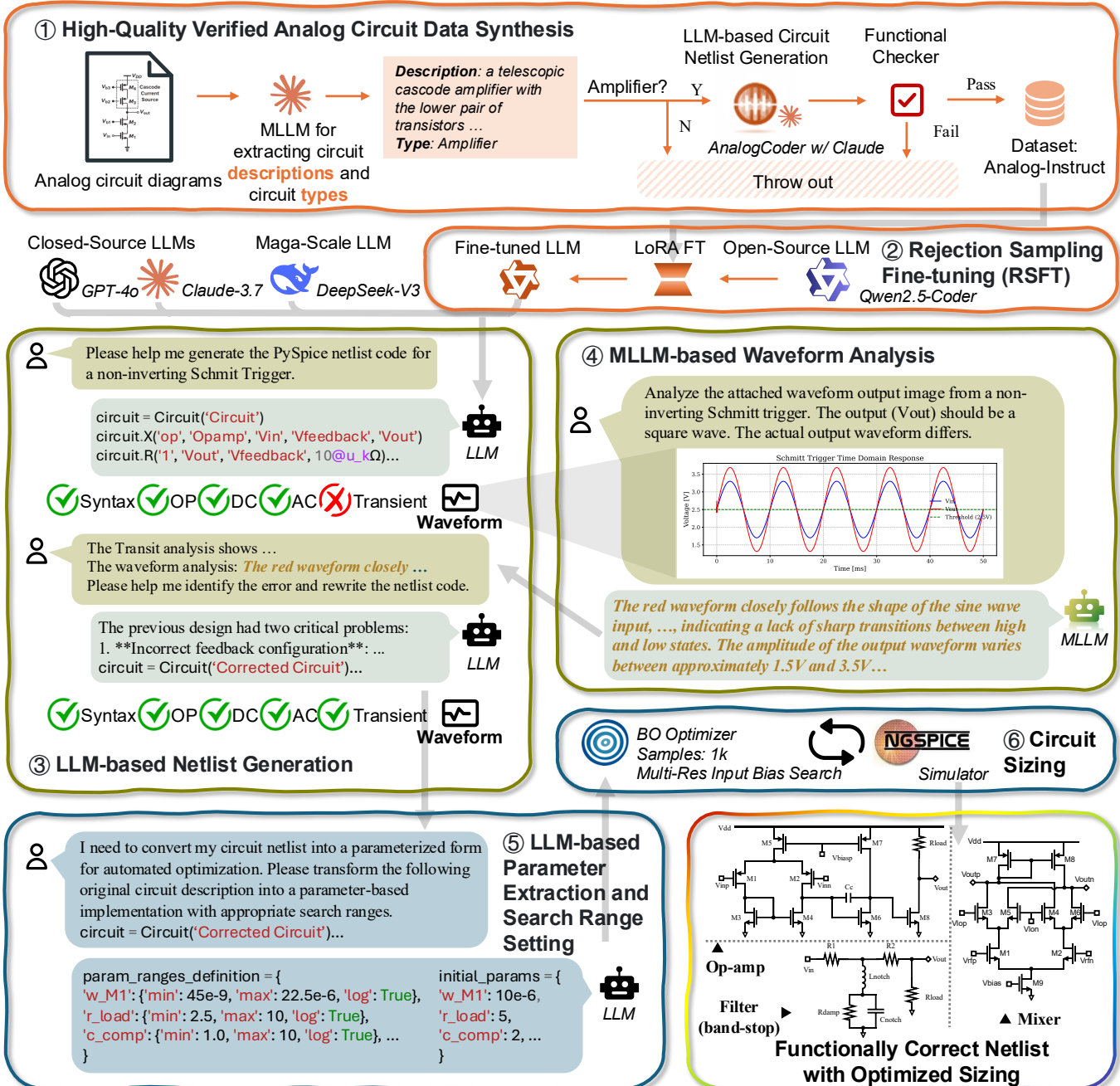


Fig. 2: **Framework of AnalogCoder-Pro.** AnalogCoder-Pro integrates circuit generation and optimization into a unified flow, comprising three main modules: (1) Rejection sampling-based fine-tuning on high-quality synthesis data (①②); (2) MLLM-enhanced netlist generation (③④); and (3) LLM-assisted circuit sizing (⑤⑥). Example circuits generated by AnalogCoder-Pro are shown at the end.

Rejection Sampling-based fine-tuning has been successfully adopted in various LLM fine-tuning pipelines, such as Llama-2 and DeepSeek-R1.

In our analog netlist generation workflow, we simulate each LLM-generated candidate netlist and use circuit-specific functional test code to validate the simulation results. By selecting only those netlists that pass functional verification for fine-tuning, we significantly improve the quality of training data, enhancing the model's ability to generate functionally correct netlists after fine-tuning.

C. Multi-modal Large Language Model

With the rapid progress of LLMs, researchers have developed Multi-modal Large Language Models (MLLMs), which can process images and text as input and generate text as output. Unlike traditional LLMs, which only understand text, MLLMs can jointly perceive and reason over visual and textual information. Representative models such as GPT-4 and Qwen-VL have demonstrated impressive capabilities in tasks that require understanding images and language, like visual question answering.

Typically, an MLLM consists of a vision encoder and a text encoder, which convert images and text into feature tokens, respectively. These tokens are concatenated and fed into the language model to predict the output sequence. Formally, given an image I and a text sequence T , the model computes:

$$\begin{aligned} z_{\text{vision}} &= E_{\text{vision}}(I), \quad z_{\text{text}} = E_{\text{text}}(T), \\ y &= \text{LM}([z_{\text{vision}}, z_{\text{text}}]) \end{aligned}$$

where E_{vision} and E_{text} denote the vision and text encoders, and LM is the large language model, and y is the predicted output sequence.

MLLMs offer unique advantages in circuit understanding and EDA applications [53], [54]. For example, engineers often analyze waveform plots to debug or optimize analog circuits, as such plots are more intuitive than raw numerical data. We provide a concrete example in Fig. 1: when samples from a distorted triangular waveform are fed into a text-based LLM, it incorrectly identifies the signal as a sine wave, exposing its fundamental limitation in interpreting numerical patterns. In contrast, MLLMs correctly recognize the triangular wave despite distortions, leveraging visual pattern recognition, rather than relying solely on numerical data. This multimodal capability significantly enhances waveform identification accuracy, crucial for effective circuit debugging and behavior validation. It thereby improves the overall efficiency and intelligence of circuit analysis and design.

III. ANALOGCODER-PRO FRAMEWORK AND METHODS

A. Overall Framework

As shown in Fig. 2, our proposed AnalogCoder-Pro is a comprehensive framework that jointly optimizes topology generation and device sizing within a unified, performance-centric flow. This flow consists of rejection sampling fine-tuning (①②), circuit netlist generation (③④), and circuit device sizing (⑤⑥).

Specifically, the overall process is driven by LLMs, which generate circuit topologies and optimize device parameters in response to user instructions. In the first stage, the LLM generates synthetic netlists, and only those validated as functionally correct through simulation are retained. These filtered netlists form a specialized dataset for continual model improvement. In the second stage, topology generation is guided by the LLM using both the existing netlist data and simulation waveform images. The MLLM analyzes the simulation waveform images and returns the results to the LLM, combining these results with the netlist information to diagnose design issues and enable iterative refinement. In the final stage, the LLM extracts circuit parameters and their search ranges, which are fed into Bayesian optimization to generate a fully functional and optimized circuit design.

B. Rejection Sampling Fine-tuning for Circuit Generation

As illustrated in ① of Fig. 2, we adopt a two-step process to construct a high-quality circuit netlist dataset for fine-tuning. To ensure unbiased performance measurement and avoid data contamination, we restrict the dataset to amplifier circuits, ensuring a clear separation between fine-tuning and test data.

In the first step, we use an MLLM to generate circuit descriptions and classify the circuit type based on circuit diagrams. For example, a generated description might be: ***Description:** A telescopic cascode amplifier with the lower pair of transistors serving as input stages and the upper cascode pair providing high output impedance while maintaining current biasing. **Type:** Amplifier.*” Next, we filter the descriptions to retain only those classified as amplifier and use them as input for netlist generation. Following the workflow of AnalogCoder [27], we verify the generated circuit netlists by testing codes to ensure they are functionally correct before including them in the dataset.

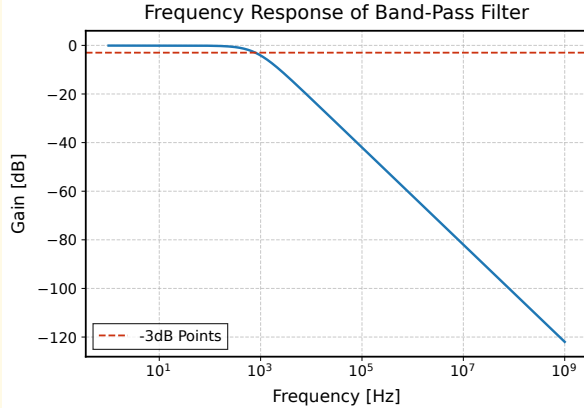
Specifically, after filtering out diagrams without input or output, we obtained 153 amplifier design descriptions from AnalogGenie [21]. For each, we used AnalogCoder to generate netlists, running up to 15 iterations until three correct netlists were found. In total, 390 high-quality netlists were produced for the analog-instruct dataset used for fine-tuning. Each entry consists of a question (following AnalogCoder’s prompts) and an answer (the design plan and corresponding netlist code).

Using this high-quality dataset, we fine-tune the open-source code-specific LLM, Qwen2.5-Coder, as illustrated in step ② of Fig. 2. To preserve the model’s general capabilities while enhancing its proficiency in analog circuit generation, we employ Low-Rank Adaptation (LoRA) [55]. The fine-tuning process is conducted exclusively on our rigorously validated dataset, ensuring reliable supervision signals and improved performance in analog circuit generation.

C. MLLM-Enhanced Circuit Netlist Generation

As shown in steps ③ and ④ of Fig. 2, our topology netlist generation mainly follows the AnalogCoder feedback-enhanced workflow. Step ③ illustrates how user requirements prompt an LLM (either a fine-tuned open-source model or a

Instruction



Analyze the attached waveform output image from a **passive band-pass filter circuit**. **Vout** should show attenuation at both low and high frequencies, with maximum amplitude occurring within a specific frequency range. The actual output waveform differs. The testbench applies a **1Hz-1GHz frequency sweep signal to Vin**.

Please provide a detailed analysis of the waveform characteristics within one paragraph, including shape, amplitude, frequency, stability, any differences from the expected pattern (e.g., DC level, decay, irregular behavior), and unusual features or distortions.

Please describe the waveform features solely based on the image.

Response

The waveform shows a frequency response that deviates significantly from expected band-pass filter behavior. Instead of exhibiting attenuation at both low and high frequencies with a peak in the middle, this response displays nearly flat gain (close to 0 dB) at low frequencies up to approximately 1 kHz, followed by a continuous monotonic roll-off at higher frequencies. The response maintains approximately 0 dB gain from 1 Hz to about 1 kHz, then begins a steady decline that reaches approximately -40 dB at 100 kHz, -80 dB at 10 MHz, and continues dropping to around -120 dB at 1 GHz. ...

Fig. 3: Example of MLLM Analyzing Frequency Response. The **blue** text highlights the circuit-specific instructions, which are adapted for different circuit types. The MLLM is prompted to analyze the frequency response image, and its response demonstrates its ability to correctly interpret the image and identify discrepancies from the expected circuit behavior.

Table II: Simulation Image Types Provided to the MLLM for Different Circuit Types

Circuit Type	Transient	AC	FFT	DC Sweep	DC Transfer
Mixer	•		•		
Comparator					
Filter		•			
Oscillator	•				
Integrator	•				
Differentiator	•				
Schmitt trigger	•				•

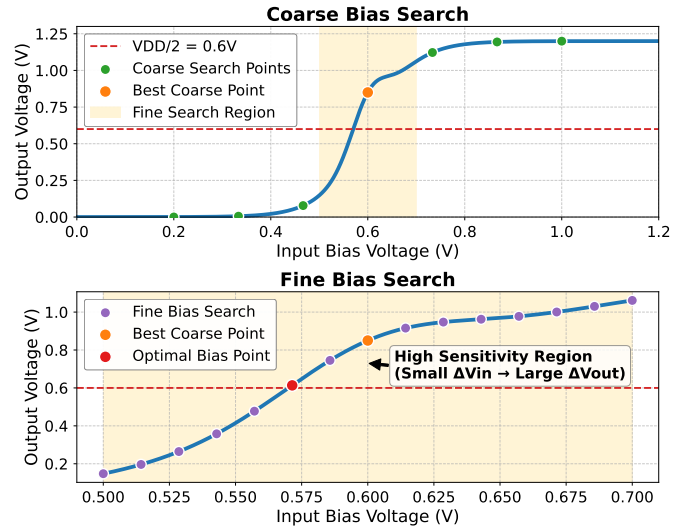


Fig. 4: Multi-Resolution Search for Input Bias. The algorithm conducts a coarse-to-fine DC sweep to automatically locate the input bias that sets the output voltage closest to $V_{DD}/2$, ensuring proper circuit biasing while reducing optimization dimensionality.

proprietary one) to generate Python code for the circuit. The generated code then undergoes syntax, OP (Operation Point), DC (Direct Current), AC (Alternating Current), and transient tests. If errors are detected, feedback is provided to the LLM so it can correct and regenerate the netlist code.

However, relying solely on textual data is insufficient for thorough circuit analysis. Therefore, we generate targeted circuit waveform images (e.g., transient, AC sweep, FFT, DC sweep, DC transfer) for each circuit type, as detailed in Table II. The waveform analysis prompts are predefined for supported circuit types. As shown in step ④ of Fig. 2, the MLLM is prompted to analyze these waveforms and provide feedback to the netlist generation LLM, along with raw error information. Fig. 3 provides an example of such an instruction-response pair for waveform image interpretation.

D. LLM-assisted Circuit Device Sizing

Upon completion of circuit netlist generation, the resulting code already contains a set of nominal parameters, such as transistor sizing, bias voltages, capacitances, and resistances. However, these default values only ensure functional correctness and often lead to suboptimal performance. To address this, we incorporate parameter tuning into our flow, as illustrated in steps ⑤ and ⑥ of Fig. 2. Specifically, in step ⑤, we instruct the LLM to automatically analyze the generated netlist, identify all tunable parameters, and determine appropriate value ranges for each based on the circuit context. The initial values are set to the nominal parameters from the netlist. The LLM then re-formats the raw netlist into a parameter-configurable template, enabling seamless integration with general optimization frameworks.

In step ⑥, we use a Bayesian Optimizer for circuit sizing. For each parameter set proposed by the optimizer, we do not directly incorporate the input voltage bias as an optimization variable. This is because the output voltage is highly sensitive to the bias point—a small change in input voltage can cause a significant variation in output voltage. To address this, we determine its optimal value through an automated multi-resolution search process. As illustrated in Fig. 4, this algorithm executes DC sweeps at progressively refined resolutions, systematically identifying the precise input voltage that biases the output voltage closest to $VDD/2$ —a condition that ensures all MOSFETs operate in their saturation region. Only after establishing this optimal bias point do we proceed with comprehensive circuit simulation to evaluate performance metrics, which subsequently provide the reward signal for the optimizer. This strategic decoupling reduces optimization space dimensionality while guaranteeing proper circuit biasing for each parameter configuration under evaluation, thereby enhancing convergence efficiency and solution quality.

IV. EXPERIMENTAL RESULTS

A. Experimental Settings

Benchmark. We follow the benchmark proposed in AnalogCoder [27], which includes 24 design tasks in 12 circuit types such as amplifiers, op-amps, and current mirrors. We extend this benchmark by adding three more circuit types: mixers, filters (high-pass, low-pass, band-pass, band-stop), and comparators, resulting in 30 design tasks across 15 types. A summary of these design tasks is shown in Table IV. Each circuit type is accompanied by functional verification code to validate the generated netlists according to simulation results.

Metrics. For the topology generation task, we use the widely adopted $Pass@1 = k/n$ metric to compute the probability that the LLM can successfully design a circuit within one trial, where k represents the number of correct generations and n is the total number of attempts. We set $n = 30$ in our experiments. Note that we use the feedback-enhanced flow, allowing each generation task to be revised up to two additional times based on error messages.

For the circuit device sizing task, we align with AnalogGenie [21], using $FoM = GBW \times C_L/\text{Power}$ as the primary optimization target. For completeness, we also evaluate Gain and GBW as additional optimization targets. Optimization is performed with 1000 samples per trial, and the best value from each run is recorded. The unified generation and optimization process is repeated 30 times, and we report the best value among all 30 trials.

Hyper-parameters. For fine-tuning, we set the learning rate to $1e-5$ and train for 20 epochs. Bayesian optimization uses a TPE sampler by the Optuna framework with 1000 samples, 25% random initialization, and multivariate sampling for parameter dependencies. All input bias sweeps are from $0.25V_{dd}$ to $0.75V_{dd}$ to avoid unreliable operating regions. LLM temperature is set to 0.5 for netlist generation and 0.0 for MLLM-based signal image analysis and parameter extraction.

Experiments are run on a server with four H800 GPUs, using the 45nm process as in AnalogGenie.

B. Rejection Sampling Fine-Tuning

We first use Claude-3.7 to extract 153 amplifier task descriptions from AnalogGenie’s circuit diagrams. Based on these, we construct two datasets: one with the original netlists provided by AnalogGenie and another with functionally verified netlists regenerated by AnalogCoder. We then fine-tune models on both datasets and compare their performance. As shown in Table III, fine-tuning on the verified dataset (RSFT) significantly improves the overall average success rate. For example, the Qwen2.5-Coder 32B model’s average success rate increases from 20.5% (base) to 30.6% (RSFT), surpassing GPT-4o-mini. To avoid data leakage, amplifier-related tasks are excluded from calculating the average success rate. Although the model still lags behind proprietary solutions on complex circuit tasks (e.g., GPT-4o), RSFT provides a cost-effective and efficient approach for circuit design, requiring only a single H800 GPU for inference.

C. MLLM-based Circuit Diagnosis and Repair

The circuit netlist generation results in Table III already incorporate error correction based on MLLM analysis of waveform images. For each LLM, we select the corresponding MLLM variant: Qwen2.5 uses Qwen2.5-VL-Max, DeepSeek-V3 uses GPT-4o (since DeepSeek does not support multi-modal inputs), and others use their own multi-modal versions.

To further assess the impact of MLLM, we conduct an ablation study by removing the MLLM component and providing only textual information for debugging. The results shown in Table V demonstrate that incorporating MLLM-based waveform analysis consistently improves circuit debugging performance across all models. Notably, Claude-3.7 achieves the most significant improvement, with its average accuracy rising from 83.8% to 90.7% when assisted by MLLM. Figure 5 presents a specific case solved by Claude-3.7, further illustrating its strong capability in interpreting waveforms and repairing circuits. Overall, these results confirm that leveraging MLLM for waveform analysis is effective for circuit generation.

D. LLM-based Unified Generation and Optimization

We evaluated the ability of LLMs to generate performance-driven analog circuit topologies using 12 distinct design instructions (see Fig. 6). We compared two prompting strategies for each circuit type: one with an explicit design objective (e.g., “Design a multi-stage op-amp topology that optimizes FoM ($GBW*CL/\text{Power}$)”) and one without (e.g., “Design a multi-stage op-amp”). As shown by the adjacent rows across each base model in Table VI, target-guided prompts consistently yield improvements in objective-specific results, confirming that the LLM can effectively incorporate optimization goals during netlist generation.

Benefiting from our multi-resolution input bias search, some circuits generated by AnalogCoder have already achieved satisfactory baseline performance with nominal size. By further

Table III: **Performance Comparison on Circuit Netlist Generation.** The best performance among the three fine-tuning methods (Base, FT, RSFT) for the same model size is marked in **bold**. **Highlighted cells** indicate the best performance in each column. All base models are implemented in our AnalogCoder-Pro framework.

Base (AnalogCoder-Pro)	Size	Amp	Inv	CM	Op	Osc	Int	Diff	Add	Sub	Sch	Comp	Mix	Filt	Avg/Type	Avg/Task	
Qwen2.5-Coder	7B	39.0	38.3	1.7	0.0	0.0	0.0	0.0	0.0	0.0	3.3	20.0	3.3	24.2	7.6	8.8	
		- FT	27.1	38.3	23.3	0.0	0.0	0.0	0.0	0.0	6.7	40.0	3.3	26.7	11.5	12.2	
		- RSFT	58.1	96.7	45.0	0.0	1.7	0.0	0.0	0.0	0.0	33.3	13.3	18.3	17.4	17.7	
Qwen2.5-Coder	14B	57.1	96.7	13.3	0.0	0.0	3.3	10.0	70.0	3.3	3.3	53.3	3.3	24.2	23.4	20.1	
		- FT	57.1	50.0	21.7	1.7	1.7	0.0	10.0	60.0	0.0	3.3	86.7	13.3	27.5	23.1	19.1
		- RSFT	70.0	100.0	41.7	0.8	0.0	0.0	13.3	90.0	3.3	0.0	33.3	3.3	32.5	26.5	24.3
Qwen2.5-Coder	32B	55.7	100.0	36.7	1.7	8.3	13.3	30.0	60.0	0.0	20.0	53.3	20.0	27.5	30.9	26.2	
		- FT	70.5	36.7	28.3	1.7	0.0	36.7	26.7	30.0	0.0	16.7	63.3	20.0	30.0	24.2	19.6
		- RSFT	71.4	100.0	45.0	0.8	3.3	66.7	93.3	30.0	6.7	23.3	46.7	10.0	16.7	36.9	30.6
GPT-4o-mini	N/A	48.6	93.3	45.0	0.0	3.3	20.0	23.3	83.3	3.3	0.0	86.7	40.0	39.2	36.5	30.3	
GPT-4o	N/A	96.2	100.0	58.3	46.7	5.0	100.0	90.0	100.0	76.7	43.3	100.0	53.3	66.7	70.0	58.4	
DeepSeek-V3	671B	99.5	100.0	80.0	48.3	20.0	96.7	100.0	100.0	93.3	40.0	100.0	66.7	84.2	77.4	66.4	
Claude-3.7	N/A	100.0	100.0	53.3	96.7	73.3	100.0	100.0	100.0	100.0	66.7	100.0	100.0	91.7	90.1	81.5	

Amp: Amplifier, **Inv:** Inverter, **CM:** Current Mirror, **Op:** Op-Amp, **Osc:** Oscillator, **Int:** Integrator, **Diff:** Differentiator, **Add:** Adder, **Sub:** Subtractor, **Sch:** Schmitt Trigger, **Comp:** Comparator, **Mix:** Mixer, **Filt:** Filter, **Avg/Type:** Average per Circuit Type (w/o Amp), **Avg/Task:** Average per Design Task (w/o Amp). We omit amplifiers for average statistics to avoid data contamination. The types that LLMs cannot successfully design are omitted.

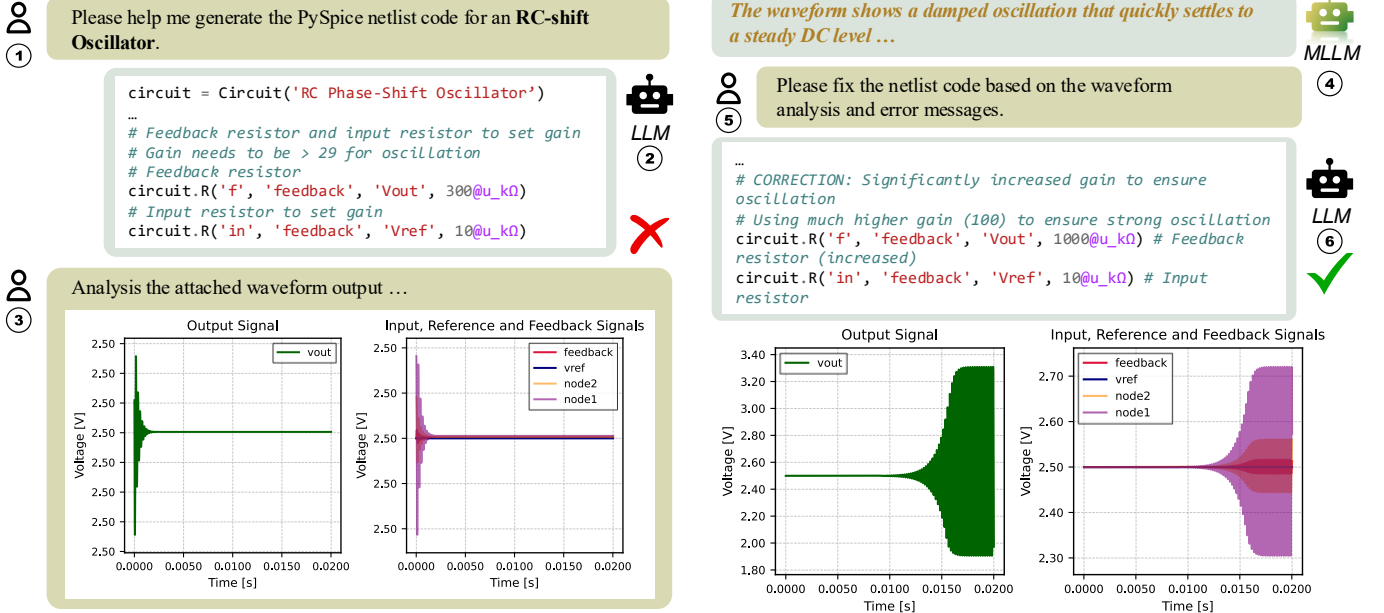


Fig. 5: **Circuit Repair via MLLM Waveform Analysis.** The MLLM interprets simulated waveform images and provides diagnostic feedback, enabling the LLM to adjust the circuit netlist and achieve the correct circuit automatically.

Table IV: **Summary of Circuit Types for Evaluation**

Type	Count	Type	Count	Type	Count
Amplifier	7	Opamp	4	Differentiator	1
Inverter	2	Oscillator	2	Adder	1
Current Mirror	2	Integrator	1	Subtractor	1
Filter	4	Schmitt trigger	1	VCO	1
Mixer	1	Comparator	1	PLL	1

leveraging the LLM to extract optimizable parameters and integrating Bayesian optimization, AnalogCoder-Pro achieves substantial performance gains compared to AnalogGenie, with up to 2× improvement in opamp FoM (see Table VI). Further-

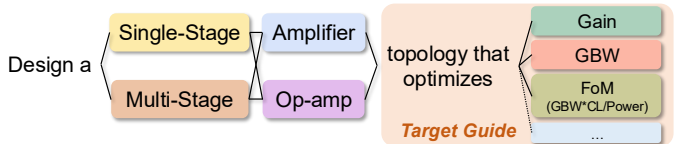


Fig. 6: **Unified Generation and Optimization Task Instructions.** All instruction paths shown are evaluated in Table VI, and the target-guided objective (e.g., Gain, GBW, or user-defined FoM) is optional for topology optimization.

more, we performed an ablation study on our multi-resolution

Table V: Performance Comparison of MLLM-Assisted Circuit Diagnosis and Repair. Each model is evaluated without and with (marked with •) MLLM assistance. **Bold** numbers indicate better performance in each pair.

Model	MLLM	Osc	Int	Diff	Sch	Comp	Mix	Filt	Avg.
Qwen2.5-Coder-32B	•	1.7 8.3	6.7 13.3	40.0 30.0	20.0 20.0	20.0 53.3	16.7 20.0	16.7 27.5	17.5 24.6
GPT-4o	•	6.7 5.0	86.7 100.0	86.7 90.0	33.3 43.3	100.0 100.0	46.7 53.3	67.5 66.7	61.1 65.5
DeepSeek-V3	•	8.3 20.0	100.0 96.7	96.7 100.0	50.0 40.0	100.0 100.0	63.3 66.7	80.8 84.2	71.3 72.5
Claude-3.7	•	70.0 73.3	100.0 100.0	100.0 100.0	26.7 66.7	100.0 100.0	100.0 100.0	91.7 91.7	84.1 90.2

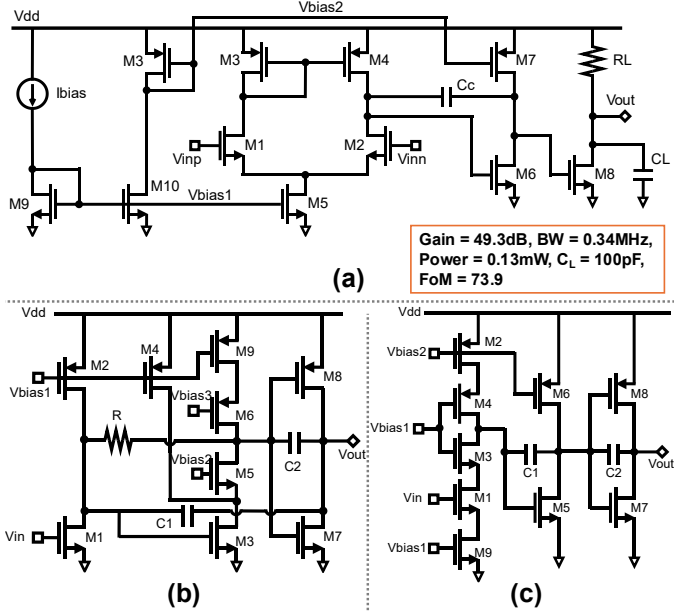


Fig. 7: Circuit topologies generated by AnalogCoder-Pro.
(a) Op-amp with the highest FoM, also evaluated in Fig. 8;
(b), (c) Amplifiers generated using FoM-guided design instructions.

input bias search, using the best FoM netlist generated by Claude-3.7 (Fig. 7(a)). For each bias determination approach, we ran the optimizer five times with different seeds. The single-resolution method used 2000 uniform steps, while the multi-resolution method used 20, 200, and 2000 steps at coarse, medium, and fine stages, respectively. As shown in Fig. 8, multi-resolution search consistently outperforms single-resolution search, fixed bias, and treating input bias as an optimizable parameter across all metrics. Additional generated amplifier topologies are shown in Fig. 7(b) and (c).

V. CONCLUSION

In this work, we introduce AnalogCoder-Pro, a unified, end-to-end framework for automated analog circuit design with multimodal LLMs. By combining functionally verified data synthesis, waveform-based debugging, and integrated performance-driven topology generation, AnalogCoder-

Pro achieves state-of-the-art performance and substantially improves success rates across diverse circuit design tasks.

REFERENCES

- [1] B. Razavi, “Design of analog cmos integrated circuits,” 2000.
- [2] G. Stehr, H. Graeb, and K. Antreich, “Performance trade-off analysis of analog circuits by normal-boundary intersection,” in *Proceedings of the 40th annual Design Automation Conference*, 2003, pp. 958–963.
- [3] D. Mueller-Gritschneider, H. Graeb, and U. Schlichtmann, “A successive approach to compute the bounded pareto front of practical multiobjective optimization problems,” *SIAM Journal on Optimization*, vol. 20, no. 2, pp. 915–934, 2009.
- [4] H. Wang, K. Wang, J. Yang, L. Shen, N. Sun, H.-S. Lee, and S. Han, “GCN-RL circuit designer: Transferable transistor sizing with graph neural networks and reinforcement learning,” in *Design Automation Conference (DAC)*, 2020.
- [5] K. Settaluri, A. Haj-Ali, Q. Huang, K. Hakhamaneshi, and B. Nikolic, “Autockt: Deep reinforcement learning of analog circuit designs,” in *Design, Automation & Test in Europe Conference & Exhibition (DATE)*, 2020.
- [6] A. F. Budak, P. Bhansali, B. Liu, N. Sun, D. Z. Pan, and C. V. Kashyap, “Dnn-opt: An rl inspired optimization for analog circuit sizing using deep neural networks,” in *Design Automation Conference (DAC)*, 2021.
- [7] A. F. Budak, D. Smart, B. Swahn, and D. Z. Pan, “Apostle: Asynchronously parallel optimization for sizing analog transistors using dnn learning,” in *Asia South Pac. Des. Autom. Conf. (ASP-DAC)*, 2023.
- [8] M. Choi, Y. Choi, K. Lee, and S. Kang, “Reinforcement learning-based analog circuit optimizer using g m/i d for sizing,” in *Design Automation Conference (DAC)*. IEEE, 2023.
- [9] Y. Li, Y. Lin, M. Madhusudan, A. Sharma, S. Sapatnekar, R. Harjani, and J. Hu, “A circuit attention network-based actor-critic learning approach to robust analog transistor sizing,” in *Workshop on Machine Learning for CAD (MLCAD)*, 2021.
- [10] Y. Oh, D. Kim, Y. H. Lee, and B. Hwang, “Cronus: Circuit rapid optimization with neural simulator,” in *Design, Automation & Test in Europe Conference & Exhibition (DATE)*, 2024.
- [11] S. Poddar, Y. Oh, Y. Lai, H. Zhu, B. Hwang, and D. Z. Pan, “Insight: Universal neural simulator for analog circuits harnessing autoregressive transformers,” in *Design Automation Conference (DAC)*, 2025.
- [12] T. McConaghay, P. Palmers, G. Gielen, and M. Steyaert, “Simultaneous multi-topology multi-objective sizing across thousands of analog circuit topologies,” in *Design Automation Conference (DAC)*, 2007.
- [13] P. Palmers, T. McConaghay, M. Steyaert, and G. Gielen, “Massively multi-topology sizing of analog integrated circuits,” in *Design, Automation & Test in Europe Conference & Exhibition (DATE)*. IEEE, 2009.
- [14] P. Veselinovic, D. Leenaerts, W. Van Bokhoven, F. Leyn, F. Proesmans, G. Gielen, and W. Sansen, “A flexible topology selection program as part of an analog synthesis system,” in *European Design and Test Conference*, 1995.
- [15] T. McConaghay, P. Palmers, G. Gielen, and M. Steyaert, “Automated extraction of expert knowledge in analog topology selection and sizing,” in *International Conference on Computer-Aided Design (ICCAD)*, 2008.
- [16] Z. Zhao and L. Zhang, “An automated topology synthesis framework for analog integrated circuits,” *IEEE Trans. Comput.-Aided Des. Integr. Circuits Syst. (TCAD)*, vol. 39, no. 12, pp. 4325–4337, 2020.
- [17] P. C. Maulik, L. R. Carley, and R. A. Rutenbar, “Integer programming based topology selection of cell-level analog circuits,” *IEEE Trans. Comput.-Aided Des. Integr. Circuits Syst.*, vol. 14, no. 4, pp. 401–412, 1995.
- [18] J. Shen, F. Yang, L. Shang, C. Yan, Z. Bi, D. Zhou, and X. Zeng, “Atom: An automatic topology synthesis framework for operational amplifiers,” *IEEE Trans. Comput.-Aided Des. Integr. Circuits Syst. (TCAD)*, 2024.
- [19] J. Lu, Y. Li, F. Yang, L. Shang, and X. Zeng, “High-level topology synthesis method for δ - σ modulators via bi-level bayesian optimization,” *IEEE Transactions on Circuits and Systems II: Express Briefs*, vol. 70, no. 12, pp. 4389–4393, 2023.
- [20] S. Poddar, A. Budak, L. Zhao, C.-H. Hsu, S. Maji, K. Zhu, Y. Jia, and D. Z. Pan, “A data-driven analog circuit synthesizer with automatic topology selection and sizing,” in *Design, Automation & Test in Europe Conference & Exhibition (DATE)*, 2024.
- [21] J. Gao, W. Cao, J. Yang, and X. Zhang, “Analoggenie: A generative engine for automatic discovery of analog circuit topologies,” in *International Conference on Learning Representations (ICLR)*, 2025.

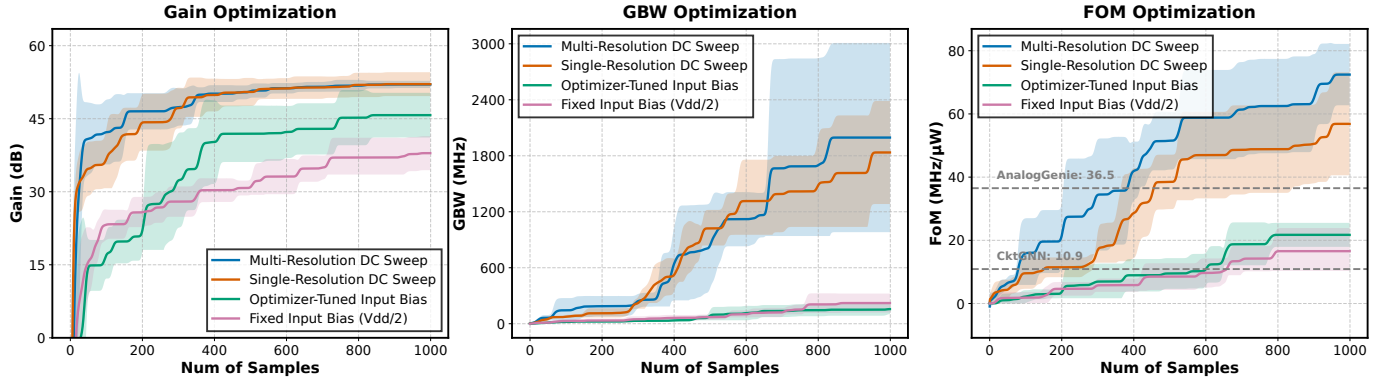


Fig. 8: **Comparison of Input Bias Voltage Selection Methods.** Each method is evaluated over 5 independent optimization runs. The proposed multi-resolution bias selection approach achieves faster and more accurate convergence to the optimal operating points, resulting in improved circuit performance metrics. The circuit topology for evaluation is shown in Fig. 7(a).

Table VI: **Performance Comparison for Unified Circuit Generation and Optimization.** For each instruction in Fig. 6, 30 netlist generation attempts are performed. Each correct netlist is optimized with 1000 samples, and the best performance among the 30 trials is reported. Maximum values are in **bold**. AnalogGenie and CktGNN results are from the original papers.

Method (# Samples)	Base Model	Target-guided ²	Single-Stage Amp Gain	Single-Stage Amp GBW	Single-Stage Amp FoM ¹	Single-Stage Opamp Gain	Single-Stage Opamp GBW	Single-Stage Opamp FoM	Multi-Stage Amp Gain	Multi-Stage Amp GBW	Multi-Stage Amp FoM	Multi-Stage Opamp Gain	Multi-Stage Opamp GBW	Multi-Stage Opamp FoM	Avg. Rank
CktGNN	GNN	•	-	-	-	-	-	-	-	-	-	-	-	-	10.9
AnalogGenie(>1k)	GPT-2	•	-	-	-	-	-	-	-	-	-	-	-	-	36.5
AnalogCoder(1)	GPT-4o	•	13.9	93.2	1.7	12.8	113.1	0.6	40.6	2076.2	5.7	18.0	154.6	0.5	10.5
	DeepSeek-V3	•	16.2	191.7	1.1	13.4	85.1	0.8	43.8	4195.4	8.8	35.5	880.8	2.4	9.1
	Claude-3.7	•	0.7	23.6	1.7	13.5	147.7	0.9	37.5	5330.6	8.5	27.8	1050.9	4.1	9.5
		•	26.2	198.5	1.0	29.7	153.5	2.6	37.5	9808.7	13.1	7.8	443.1	4.2	7.7
AnalogCoder-Pro(1k)	GPT-4o	•	16.0	49.4	1.9	14.5	130.0	1.1	35.8	314.8	1.2	67.9	2384.8	12.1	8.2
	DeepSeek-V3	•	30.5	157.4	1.0	23.1	13.7	1.1	0.0	4081.3	165.9	40.0	899.0	0.5	8.2
	Claude-3.7	•	18.6	416.8	2.0	20.6	299.1	2.9	56.3	23111.9	133.2	33.3	1406.1	9.5	4.9
		•	18.9	443.3	2.4	20.4	260.3	3.6	55.7	35873.3	124.0	50.2	1122.2	37.4	4.5
AnalogCoder-Pro(1k)	DeepSeek-V3	•	16.1	50.4	1.9	20.5	279.9	3.0	55.9	22579.2	127.3	36.4	2346.0	14.1	5.8
	Claude-3.7	•	27.5	418.8	2.5	36.2	363.3	14.5	56.4	41316.7	185.7	36.6	2243.9	36.2	2.5
		•	16.1	100.6	1.9	27.8	281.3	8.5	53.2	5298.2	135.1	67.9	6279.4	43.4	4.7
		•	45.3	413.3	3.2	39.2	266.6	7.4	46.1	17366.0	413.2	74.9	3193.0	73.9	2.6

¹ Gain (dB) = $20 \times \log_{10}(V_{out}/V_{in})$, GBW (MHz) = Gain (linear) \times Bandwidth, FoM (MHz·pF/µW) = GBW \times C_L/Power , where $C_L = 100\text{ pF}$.

² Target-guided design indicates that specific design objectives (e.g., maximizing the Figure of Merit, FoM) were set for the LLM, as shown in Fig. 6.

[22] Z. Dong, W. Cao, M. Zhang, D. Tao, Y. Chen, and X. Zhang, “Cktggn: Circuit graph neural network for electronic design automation,” in *International Conference on Learning Representations (ICLR)*, 2023.

[23] C. Liu, Y. Liu, Y. Du, and L. Du, “Ladac: Large language model-driven auto-designer for analog circuits,” *Authorea Preprints*, 2024.

[24] Y. Yin, Y. Wang, B. Xu, and P. Li, “Ado-llm: Analog design bayesian optimization with in-context learning of large language models,” in *International Conference on Computer-Aided Design (ICCAD)*, 2024.

[25] C.-C. Chang, Y. Shen, S. Fan, J. Li, S. Zhang, N. Cao, Y. Chen, and X. Zhang, “Lamagic: Language-model-based topology generation for analog integrated circuits,” *arXiv preprint arXiv:2407.18269*, 2024.

[26] C.-C. Chang, W.-H. Lin, Y. Shen, Y. Chen, and X. Zhang, “Lamagic2: Advanced circuit formulations for language model-based analog topology generation,” in *Forty-second International Conference on Machine Learning*, 2025.

[27] Y. Lai, S. Lee, G. Chen, S. Poddar, M. Hu, D. Z. Pan, and P. Luo, “Analogcoder: Analog circuit design via training-free code generation,” in *AAAI Conference on Artificial Intelligence (AAAI)*, 2025.

[28] D. Vungarala, S. Alam, A. Ghosh, and S. Angizi, “Spicepilot: Navigating spice code generation and simulation with ai guidance,” *arXiv preprint arXiv:2410.20553*, 2024.

[29] D. V. Kochar, H. Wang, A. Chandrakasan, and X. Zhang, “Ledro: Llm-enhanced design space reduction and optimization for analog circuits,” *arXiv preprint arXiv:2411.12930*, 2024.

[30] Z. Chen, J. Huang, Y. Liu, F. Yang, L. Shang, D. Zhou, and X. Zeng, “Artisan: Automated operational amplifier design via domain-specific large language model,” in *Design Automation Conference (DAC)*, 2024.

[31] C. Liu, W. Chen, A. Peng, Y. Du, L. Du, and J. Yang, “Ampagent: An llm-based multi-agent system for multi-stage amplifier schematic design from literature for process and performance porting,” *arXiv*, 2024.

[32] J. Shen, Z. Chen, J. Zhuang, J. Huang, F. Yang, L. Shang, Z. Bi, C. Yan, D. Zhou, and X. Zeng, “Atelier: An automated analog circuit design framework via multiple large language model-based agents,” *Authorea Preprints*, 2024.

[33] H. Zhang, S. Sun, Y. Lin, R. Wang, and J. Bian, “Analogxpert: Automating analog topology synthesis by incorporating circuit design expertise into large language models,” *arXiv preprint*, 2024.

[34] J. Bhandari, V. Bhat, Y. He, H. Rahmani, S. Garg, and R. Karri, “Masala-chai: A large-scale spice netlist dataset for analog circuits by harnessing ai,” 2025.

[35] J. Gao, W. Cao, and X. Zhang, “Analogenie-lite: Enhancing scalability and precision in circuit topology discovery through lightweight graph modeling,” in *Forty-second International Conference on Machine Learning (ICML)*, 2025.

- [36] Q. Li, S. Hong, J. Gao, X. Zhang, T. Lan, and W. Cao, “Analogfed: Federated discovery of analog circuit topologies with generative ai,” 2025.
- [37] J. Blocklove, S. Garg, R. Karri, and H. Pearce, “Chip-chat: Challenges and opportunities in conversational hardware design,” in *Workshop on Machine Learning for CAD (MLCAD)*. IEEE, 2023.
- [38] M. Liu, T.-D. Ene, R. Kirby, C. Cheng, N. Pinckney, R. Liang, J. Alben, H. Anand, S. Banerjee, I. Bayraktaroglu *et al.*, “Chipnemo: Domain-adapted llms for chip design,” *arXiv preprint*, 2023.
- [39] S. Liu, W. Fang, Y. Lu, J. Wang, Q. Zhang, H. Zhang, and Z. Xie, “Rtlcoder: Fully open-source and efficient llm-assisted rtl code generation technique,” *IEEE Trans. Comput.-Aided Des. Integr. Circuits Syst.*, 2024.
- [40] S. Thakur, B. Ahmad, H. Pearce, B. Tan, B. Dolan-Gavitt, R. Karri, and S. Garg, “Verigen: A large language model for verilog code generation,” *ACM Transactions on Design Automation of Electronic Systems (TODAES)*, vol. 29, no. 3, pp. 1–31, 2024.
- [41] Y. Zhao, D. Huang, C. Li, P. Jin, M. Song, Y. Xu, Z. Nan, M. Gao, T. Ma, L. Qi *et al.*, “Codev: Empowering llms with hdl generation through multi-level summarization,” *arXiv preprint arXiv:2407.10424*, 2024.
- [42] Y. Zhu, D. Huang, H. Lyu, X. Zhang, C. Li, W. Shi, Y. Wu, J. Mu, J. Wang, Y. Zhao *et al.*, “Codev-r1: Reasoning-enhanced verilog generation,” *arXiv preprint arXiv:2505.24183*, 2025.
- [43] M. Akyash, K. Azar, and H. Kamali, “Rtl++: Graph-enhanced llm for rtl code generation,” *arXiv preprint arXiv:2505.13479*, 2025.
- [44] M. Liu, Y.-D. Tsai, W. Zhou, and H. Ren, “Craftrtl: High-quality synthetic data generation for verilog code models with correct-by-construction non-textual representations and targeted code repair,” *arXiv preprint*, 2024.
- [45] C. Deng, Y.-D. Tsai, G.-T. Liu, Z. Yu, and H. Ren, “Scalertl: Scaling llms with reasoning data and test-time compute for accurate rtl code generation,” *arXiv preprint arXiv:2506.05566*, 2025.
- [46] H. Wu, Z. He, X. Zhang, X. Yao, S. Zheng, H. Zheng, and B. Yu, “Chateda: A large language model powered autonomous agent for eda,” *IEEE Trans. Comput.-Aided Des. Integr. Circuits Syst. (TCAD)*, 2024.
- [47] H. Chen, M. Liu, B. Xu, K. Zhu, X. Tang, S. Li, Y. Lin, N. Sun, and D. Z. Pan, “Magical: An open-source fully automated analog ic layout system from netlist to gdsii,” *IEEE Design & Test*, 2020.
- [48] G. Chen, K. Zhu, S. Kim, H. Zhu, Y. Lai, B. Yu, and D. Z. Pan, “Llm-enhanced bayesian optimization for efficient analog layout constraint generation,” *arXiv preprint*, 2024.
- [49] P. Mangalagiri, L. Qian, F. Zafar, P. Mosalikanti, P. Chang, A. Kurian, and V. Saripalli, “Cdls: Constraint driven generative ai framework for analog layout synthesis,” in *Design Automation Conference*, 2024.
- [50] A. Hammoud, C. Goyal, S. Pathen, A. Dai, A. Li, G. Kielian, and M. Saligane, “Human language to analog layout using glayout layout automation framework,” in *International Symposium on Machine Learning for CAD (MLCAD)*, 2024.
- [51] Z. Zhao and L. Zhang, “Deep reinforcement learning for analog circuit structure synthesis,” in *Design, Automation & Test in Europe Conference & Exhibition (DATE)*, 2022.
- [52] Zhao, Zhenxin and Zhang, Lihong, “Graph-grammar-based analog circuit topology synthesis,” in *IEEE International Symposium on Circuits and Systems (ISCAS)*, 2019, pp. 1–5.
- [53] W. Fang, S. Liu, J. Wang, and Z. Xie, “Circuitfusion: multimodal circuit representation learning for agile chip design,” in *International Conference on Learning Representations (ICLR)*, 2025.
- [54] K. Chang, Z. Chen, Y. Zhou, W. Zhu, K. Wang, H. Xu, C. Li, M. Wang, S. Liang, H. Li *et al.*, “Natural language is not enough: Benchmarking multi-modal generative ai for verilog generation,” in *International Conference on Computer-Aided Design (ICCAD)*, 2024.
- [55] E. J. Hu, Y. Shen, P. Wallis, Z. Allen-Zhu, Y. Li, S. Wang, L. Wang, W. Chen *et al.*, “Lora: Low-rank adaptation of large language models,” in *International Conference on Learning Representations (ICLR)*, 2022.